Received: 20 November 2024 | Accepted: 14 March 2025

DOI: 10.1111/2041-210X.70075

Methods in Ecology and Evolution

RESEARCH ARTICLE

Toward a unified approach to modelling adaptation among demographers and evolutionary ecologists

Joanie Van de Walle[1,2] | **Jimmy Garnier**[3] | **Timothée Bonnet**[4] | **Stephanie Jenouvrier**[1]

[1]Biology Department, Woods Hole Oceanographic Institution, Woods Hole, Massachusetts, USA

[2]Department of Fisheries and Oceans Canada, Maurice Lamontagne Institute, Mont-Joli, Quebec, Canada

[3]LAMA, CNRS-University de Grenoble Alpes, Université de Savoie Mont Blanc, UMR-5127, Chambéry, France

[4]Centre d'Etudes Biologiques de Chizé, CNRS-La Rochelle University UMR-7372, Villiers en Bois, France

Correspondence
Stephanie Jenouvrier
Email: sjenouvrier@whoi.edu

Funding information
National Science Foundation, Grant/Award Number: NSFGEO-NERC 1951500 and ORCC NSF 2222057

Handling Editor: Aldo Compagnoni

Abstract

1. Demographic and evolutionary modelling approaches are critical to understanding and projecting species responses to global environmental changes. Population matrix models have been a favoured tool in demography, but until recently, they failed to account for short-term evolutionary changes. Evolutionary-explicit demographic models remain computationally intensive, difficult to use and have yet to be widely adopted for empirical studies. Researchers focusing on short-term evolution often favour individual-based simulations, which are more flexible but less transferable and computationally efficient. Limited communication between fields has led to differing perspectives on key issues, such as how life-history traits affect adaptation to environmental change.
2. We develop a new EvoDemo hyperstate matrix population model (EvoDemo-Hyper MPM) that incorporates the genetic inheritance of quantitative traits, enabling fast computation of evolutionary and demographic dynamics. We evaluate EvoDemo-Hyper MPM against individual-based simulations and provide analytical approximations for adaptation rates across six distinct scales in response to selection. We show that different methods yield equivalent results for the same biological scenario, although semantic differences between fields may obscure these similarities.
3. Our results demonstrate that EvoDemo-Hyper MPM provides accurate, computationally efficient solutions, closely matching outcomes from individual-based simulations and analytical approximations under similar biological conditions. Adaptation rates per generation remain constant across species when selection acts on fertility but vary with other vital rates. Adaptation per time decreases with generation time unless selection targets adult survival, where intermediate life histories adapt fastest. Rates per generation, defined as the relative change in individual fitness, remain constant across species and vital rates.
4. We discuss that no general prediction emerges about which species or life-history traits yield higher adaptation rates, as outcomes depend on life cycles, vital rates

All authors contributed equally to this work.

and the definition used. We provide Matlab and R code to support the application of our EvoDemo-Hyper MPM.

KEYWORDS
adaptive evolution, evolutionary demography, hyperstate matrix model, life-history strategies, quantitative genetics, slow-fast continuum

1 | INTRODUCTION

Understanding how populations respond to environmental changes is essential for effective conservation. For instance, changes in range, immigration or dispersion rates and life-history traits in response to environmental changes can affect population growth and persistence (Bellard et al., 2012; Doak & Morris, 2010; Parmesan & Yohe, 2003). In particular, changes in population growth in response to environmental changes can be mediated by phenotypic changes through different mechanisms: changes in demographic structure, phenotypic plasticity and contemporary evolution (Chevin et al., 2012; Gonzalez et al., 2013; van Benthem et al., 2017). Among these, contemporary evolution in response to selection is a particularly powerful mechanism, enabling populations to adapt to environmental change over both short and long timescales (Gonzalez et al., 2013). However, integrating demographic and evolutionary perspectives remains a significant challenge. Bridging these perspectives is crucial for improving predictions of species' responses to global change, as populations with a greater capacity for adaptive responses are more likely to persist over time (Berteaux et al., 2004; Jenouvrier & Visser, 2011).

Integral projection models (IPMs) which are an extension of matrix population models that include continuous state variables, have been widely used to model population responses to selection acting on continuous phenotypic traits in terms of future phenotypic distribution and stage abundance (Easterling et al., 2000). IPMs allow efficient computation of population properties, but their original formulation did not account for evolution or include explicit genetic dimensions. Recent advances introduced inheritance and evolutionary dynamics into IPMs (Childs et al., 2016; Coulson et al., 2017). However, these improvements involve nonlinear iterative steps that reduce computational efficiency and limit their applicability.

Incorporating adaptive evolution into matrix population models (MPMs) requires additional dimensions to capture both phenotypic traits and genetic inheritance. Multitrait population projection matrices (MPPMs) address genetic variance and multiple vital rates (Coste & Pavard, 2020). However, they often lack explicit trait inheritance within a quantitative genetic framework, limiting their applicability for evolutionary research. Here, we propose using hyperstate matrix models (Roth & Caswell, 2016), which extend vec-permutation models (Hunter & Caswell, 2005) to efficiently incorporate evolutionary processes and develop a new EvoDemo hyperstate matrix population model (EvoDemo-Hyper MPM).

In parallel, evolutionary quantitative geneticists have focused on predicting phenotypic changes through genetic processes, using mixed models to estimate genetic parameters and sometimes individual-based models (IBMs) to study population-level consequences of evolutionary dynamics (Haaland et al., 2023; Lachs et al., 2024; Lamarins et al., 2022; Postuma et al., 2020; Rees & Ellner, 2019; Xuereb et al., 2021). Although IBMs can accommodate complex demographic processes, they are time-consuming to develop, less transferable and computationally demanding compared to matrix models (Grimm & Railsback, 2005; Grimm, 1999).

These two modelling schools, evolutionary quantitative geneticists with IBMs versus demographers with matrix-based approaches (MPMs and IPMs) have evolved largely independently and have sometimes produced different results about the importance of evolution in short-term population dynamics. For instance, studies on bighorn sheep responses to trophy hunting have yielded contrasting results (Hedrick et al., 2014; Janeiro et al., 2017; Pelletier, 2019; Traill et al., 2014) in part because IPMs may underestimate how phenotypic differences accumulate over an individual's lifetime and are transmitted across generations (Chevin, 2015).

Demographers emphasize the importance of considering the life cycle, particularly a species' position along the slow-fast continuum of life histories (Chevin, 2015; Compagnoni et al., 2021; Paniw et al., 2018; Salguero-Gómez, 2017). Faster-lived species with shorter generation times and rapid population growth rates are expected to adapt more quickly to environmental change (Vedder et al., 2013). In contrast, evolutionary ecologists focus on predicting adaptation through the variance–covariance properties of traits and individual fitness, using tools such as the breeder's equation, the secondary theorem of selection or Fisher's fundamental theorem of natural selection (Queller, 2017). Although these approaches may seem different, quantitative evolutionary genetics inherently incorporates life cycle dynamics (Barfield et al., 2011) and aligns with demographic principles (Fisher, 1930). However, semantic differences between fields can cause confusion and hinder collaboration.

A key distinction between these frameworks lies in the time units used. Quantitative geneticists typically predict responses to selection per generation (Lynch & Walsh, 1998), whereas demographers focus on population dynamics over intervals corresponding to life-stage transitions, often annually (Caswell, 2000). This difference comes from the tools used: the breeder's equation predicts changes from generation to generation, while Leslie matrices track life-stage transitions and reproductive events over time. Although converting between these time units is straightforward,

it is not always applied in the academic literature, leading to misinterpretations.

Another difference involves how selection is quantified. In quantitative genetics, selection is expressed on the scale of relative fitness, defined as individual fitness divided by mean fitness. In contrast, demography uses regression parameters to relate traits to vital rates (e.g. survival, fertility), treating the regression slopes as indicators of selection. Additionally, non-Gaussian link functions (e.g. logit or Poisson) complicate the back-transformation of regression parameters to relative fitness scales, adding further discrepancies between the fields (de Villemereuil et al., 2016).

In this study, we integrate perspectives from demography, evolutionary genetics and mathematics by developing a matrix population model that explicitly incorporates evolutionary processes: EvoDemo-Hyper MPM. Our model predicts genetic adaptation rates for five species along the slow-fast life-history continuum, highlighting how evolutionary responses vary depending on which vital rate is under selection, with life history influencing both generation time and adaptation rates. We compare the predictions of our model with those of a similarly parameterized IBM and analytical approximations. Additionally, we express adaptation rates using six definitions, capturing different time frames and selection measures across research communities. Our findings indicate that the matrix model, IBM and analytical approaches give similar results on a common scale, but no general prediction can be made on which species or life-history trait adapts faster; it depends on the life cycle, vital rates under selection and definition choice.

2 | METHODS

In the following sections, we present methods for the construction of the evolutionary matrix population model: EvoDemo-Hyper MPM. Appendix S1 describes a corresponding Individual-Based Model. Both models are based on the same basic life cycle from which we simulated five different species with contrasted life histories. The IBM is a stochastic model that tracks each individual separately over time, whereas the EvoDemo-Hyper is a deterministic model that tracks the proportion of individuals in any given class over time. Since selection acts on individuals, IBMs incorporate selection and evolutionary processes more explicitly. Comparing the EvoDemo-Hyper with a similarly parameterized IBM allows us to validate the correct implementation of selection and genetic transmission in the EvoDemo-Hyper.

2.1 | Life cycle

The stage-structured life cycle (Figure 1) consists of juveniles (J) and adults (A). Annual transitions occur from time t to $t+1$. The survival probabilities of juveniles and adults are S_J and S_A. Juveniles at time t mature and become adults with probability γ at time $t+1$, or remain juveniles with probability $(1-\gamma)$ at time $t+1$, both given

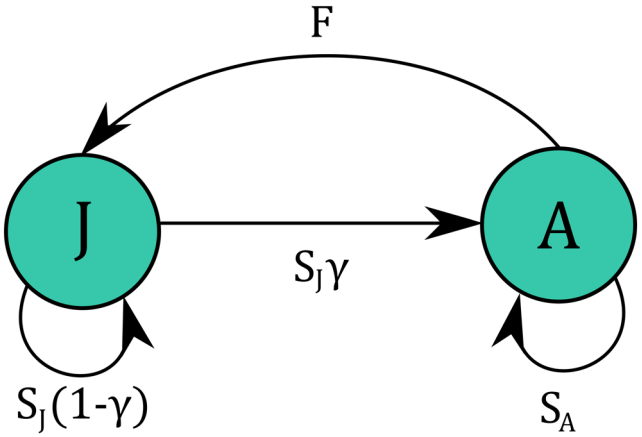

FIGURE 1 Life cycle graph of the population models.

survival. For a pre-breeding census, fertility (F) indicates the per capita rate of contribution from adults to juveniles annually, calculated as $F = f \times SJ$, with f being the annual number of offspring produced per capita (Appendix S2). An equal sex ratio for the offspring is assumed at birth. This life cycle simulates species with diverse life-history strategies (Neubert & Caswell, 2000). We model five species with increasing generation time (Table 1), mapping them along the slow-fast life-history continuum (Salguero-Gómez et al., 2016). They vary in age at first reproduction (early vs. late) and lifespan (short vs. long) (Neubert & Caswell, 2000). We also consider differences in reproductive strategies (semelparous vs. iteroparous) (Neubert & Caswell, 2000; Salguero-Gómez et al., 2016). These species illustrate a range of lifespan and reproductive variations (Table 1). Species 1 features rapid development, a single lifetime reproductive event and high fecundity, akin to annual plants and insects. Species 2 is a short-lived iteroparous species with limited offspring per time unit, similar to small mammals and birds. Species 3 spans several years, producing one offspring per time unit, like some deer. Conversely, species 4 and 5 are long-lived with delayed reproduction and low breeding output, resembling some primates or larger species like whales and albatrosses.

2.2 | Phenotypic variation, heritability and selective pressure on vital rates

Under a simple quantitative genetic infinitesimal model, the phenotype of an individual, z, can be decomposed into a population mean, an additive genetic deviation, termed the breeding value and an environmental deviation (Falconner & Mackay, 1996). The change in mean breeding values over time represents the genetic evolution of the quantitative trait considered. The variance in breeding values is the additive genetic variance ($\mathbf{V}_A$), whereas the variance in environmental deviations is the environmental variance ($\mathbf{V}_E$). The sum of the two is the phenotypic variance of a trait ($\mathbf{V}_P$), with $\mathbf{V}_P = \mathbf{V}_A + \mathbf{V}_E$. Narrow-sense heritability, denoted h^2, is the proportion of the phenotypic variance that can be attributed to inherited genetic factors, and is calculated as $h^2 = \mathbf{V}_A / \mathbf{V}_P$.

Parameter	Species 1	Species 2	Species 3	Species 4	Species 5
Fertility (F)	10.9868	4.9958	0.9987	0.3004	0.2286
Adult survival (S_A)	0.0365	0.2000	0.8000	0.9300	0.9500
Juvenile survival (S_J)	0.0965	0.2500	0.3850	0.5050	0.8000
Maturation rate (γ)	0.9000	0.5720	0.4000	0.3000	0.0700
λ	1.0000	1.0000	1.0000	1.0000	1.0000
T	2.0476	2.3698	6.3004	15.7521	23.9042

TABLE 1 Demographic parameters for the five species used in the simulations along with demographic characteristics. λ is population growth rate and T is generation time.

We explore four selection pathways targeting specific vital rates: juvenile survival S_J, adult survival S_A, fertility F and maturation γ. Selection on juvenile survival S_J, adult survival S_A or maturation γ is modulated by parameter β following a logit distribution (Appendix S3, Figure S4). For fertility F, selection is modulated by parameter β using a Poisson distribution, except for long-lived species with one offspring annually, for which fertility is modelled with logit functions. In both scenarios, parameter β indicates the strength of selective pressure on the link scale (logit or log).

2.3 | Parameter values

Vital rate values (Table 1) ensured stable equilibrium growth rates for each species ($\lambda = 1$) before selective pressures. We projected the population assuming a phenotypic variance of 1, additive genetic variance 0.2 and selective pressure 0.15. These values for $\mathbf{V}_P$ and $\mathbf{V}_A$ suggest moderate heritability (Postma, 2014). The value of β isn't directly comparable to empirical standardized selection gradients due to scale differences across species and vital rates. With heritability 0.2, observed adaptation rates per generation align with empirical gradient estimates of 0.25, fitting within empirical ranges (Kingsolver et al., 2012). Results for other parameters are described in Appendix S3. Adaptation rate magnitudes depend on $\mathbf{V}_A$ and β, yet species and vital rate differences are consistent (Figure S11).

2.4 | Principle of adaptation rate: Theoretical derivations

Adaptation rate is determined by the change in mean phenotype $\bar{z}$ over time $\Delta\bar{z}_t$. We analyse and compare adaptation rates under selective pressures on the four vital rates for each of five species. This involved eight calculation methods, varying by the time unit (year *vs* or generation) and selection unit.

2.4.1 | Rate of adaptation per unit of time, $\mathbf{RA_T}$

In the Fisher infinitesimal model Fisher (1918), the additive genetic variance stays nearly constant over time, close to $\mathbf{V}_A$. As changes in $\mathbf{V}_E$ were not modelled, the phenotypic variance also remains stable, close to $\mathbf{V}_P$. Thus, we calculate the adaptation rate per time unit $\mathbf{RA_T}$ using Lande's equation (Bulmer, 1980; Lande, 1979):

$$\mathbf{RA_T} = \Delta\bar{z}_t \approx \mathbf{V}_A\delta, \tag{1}$$

with

$$\delta = \frac{\partial \ln(\bar{\lambda})}{\partial \bar{z}_t} \tag{2}$$

which can also be written as:

$$\mathbf{RA_T} = h^2\mathbf{V}_P\frac{1}{\bar{\lambda}}\frac{\partial\bar{\lambda}}{\partial\bar{z}_t}. \tag{3}$$

In addition, when the phenotypic variance in the population is not too large, the mean growth rate $\bar{\lambda}$ is well approximated by the growth rate λ at equilibrium of a monomorphic population with trait $\bar{z}$.

The selection gradient in the population is thus approximated using the sensitivity matrix $\mathbf{S}$ associated to the growth rate λ and the variation of the vital rate with respect to the phenotype, so that $\left(\mathbf{S} = \frac{\partial\bar{\lambda}}{\partial\bar{z}_t}\right)$. The sensitivity matrix $\mathbf{S}$ is described by

$$\mathbf{S} = \frac{vw^\top}{v^\top w}, \quad \text{with } v = \begin{pmatrix} S_J\gamma \\ \lambda - S_J(1-\gamma) \end{pmatrix}, w = \begin{pmatrix} F \\ \lambda - S_J(1-\gamma) \end{pmatrix},$$

where v and w are the left and right eigenvectors associated with the eigenvalue λ of the projection matrix $\widetilde{\mathbf{A}} = \widetilde{\mathbf{U}} + \widetilde{\mathbf{F}}$ at the mean trait $\bar{z}$. The projection matrices $\widetilde{\mathbf{U}}$ and $\widetilde{\mathbf{F}}$ are defined by the life cycle in Figure 1 (see Equations (13) and (16)).

2.4.2 | Rate of adaptation per generation unit, $\mathbf{RA_G}$

The evolution of the mean phenotype can also be measured per generation time T. For a monomorphic population, generation time is defined by Bienvenu and Legendre (2015)

$$T = \frac{\lambda v^\top w}{v^\top \mathbf{R} w} = \frac{\lambda v^\top w}{v_1 w_2 F}. \tag{4}$$

The rate of adaptation per generation time is linked to the rate of adaptation per unit of time as follows

$$\mathbf{RA_G} = \mathbf{RA_T}\,T. \tag{5}$$

Here, the sensitivity matrix $\mathbf{S}$ is replaced by the following sensitivity matrix per generation $\mathbf{S}_T$ defined by

$$\mathbf{S}_T = \mathbf{S}T = \bar{\lambda}\frac{vw^\top}{v^\top \mathbf{R}w} = \bar{\lambda}\frac{vw^\top}{v_1 w_2 F}.$$

2.4.3 | Rates of adaptation per unit of vital rate, $\mathbf{RA}_{\mathbf{TS}\theta}$ and $\mathbf{RA}_{\mathbf{GS}\theta}$

The rates of adaptation can also be measured in units of vital rate, specifically based on the response of the vital rate under selection. These rates are denoted as $\mathbf{RA}_{\mathbf{TS}\theta}$ when expressed per unit of time and $\mathbf{RA}_{\mathbf{GS}\theta}$ when expressed in terms of generation time. They are calculated as follows

$$\mathbf{RA}_{\mathbf{TS}\theta} = \frac{\mathbf{RA}_\mathbf{T}}{V_\theta} \text{ and } \mathbf{RA}_{\mathbf{GS}\theta} = \frac{\mathbf{RA}_\mathbf{G}}{V_\theta}, \quad \text{where } V_\theta = \frac{\partial \ln(\theta)}{\partial \bar{z}_t} = \frac{1}{\theta}\frac{\partial \theta}{\partial \bar{z}_t}, \tag{6}$$

where V_θ is the relative rate of change in the vital rate θ of interest.

2.4.4 | Rates of adaptation per unit of fitness

The selection units can be characterized as the proportional rate of variation in an individual's fitness. Individual fitness can be measured as the average lifetime reproductive success, or the net reproductive rate R_0, which is defined for our simple life cycle as

$$R_0 = \frac{FS_J\gamma}{(1-S_A)(1-S_J(1-\gamma))}. \tag{7}$$

The rate of adaptation over time, denoted by $\mathbf{RA}_{\mathbf{TSR}_0}$ and the rate of adaptation per generation, denoted by $\mathbf{RA}_{\mathbf{GSR}_0}$, measured per unit of individual fitness, are given by

$$\mathbf{RA}_{\mathbf{TSR}_0} = \frac{\mathbf{RA}_\mathbf{T}}{V_{R_0}} \text{ and } \mathbf{RA}_{\mathbf{GSR}_0} = \frac{\mathbf{RA}_\mathbf{G}}{V_{R_0}}, \quad \text{where } V_{R_0} = \frac{\partial \ln(R_0)}{\partial \bar{z}_t} = \frac{1}{R_0}\frac{\partial R_0}{\partial \bar{z}_t} \tag{8}$$

and V_{R_0} is the relative change in individual fitness.

2.5 | EvoDemo hyperstate matrix population model

Our population model, based on the hyperstate model formulation Roth and Caswell (2016), includes three dimensions ($m = 3$) (Figure 2). Individuals are classified by stage (i), breeding value (j) and phenotype (k). The first dimension (i) ranges from 1 to s, the second (j) from 1 to b and the third (k) from 1 to p. This allows tracking of breeding values and phenotypes. The life cycle has two stages ($s = 2$). Breeding values and phenotypes are assumed to be centered at zero, ranging from − 4 to 4. They are divided into 40 classes ($b = p = 40$), which provides a good balance between computational efficiency and accurate discretization, the latter requiring $b \geq 4/\sqrt{h^2\mathbf{V}_P} \approx 9$. Note that alternative numbers of classes could have been used.

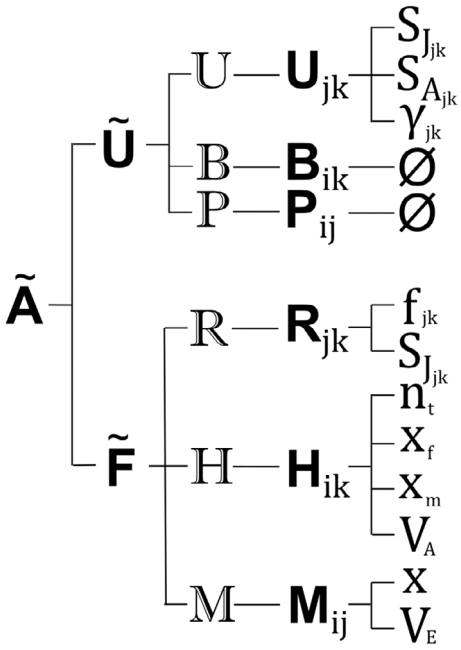

FIGURE 2 Schematic representation of the $\tilde{\mathbf{A}}$ matrix and its constituents. Note that Ø means that those matrices contain no specific parameters; they are identity matrices.

The population vector $\mathbf{n}_t$ consists of the number of individuals $n_{i,j,k}$ in each stage i, categorized by breeding value class j and phenotype class k. Phenotypes are grouped within breeding values, and breeding values are grouped within stages. Our model projects this population vector from time t to $t+1$ using the projection matrix $\tilde{\mathbf{A}}[\mathbf{n}_t]$. Although the model is centered on females, it extends to a two-sex formulation to include the distribution of male breeding values, thus accounting for genetic transmission, assuming a similar structure for both male and female populations. The dynamic of the population is given by

$$\mathbf{n}_{t+1} = \tilde{\mathbf{A}}[\mathbf{n}_t]\mathbf{n}_t. \tag{9}$$

The matrix $\tilde{\mathbf{A}}$ can be broken down into the matrices $\tilde{\mathbf{U}}$ and $\tilde{\mathbf{F}}$ (Figure 2), which represent the transition of living individuals and the production of offspring, respectively.

$$\tilde{\mathbf{A}}[\mathbf{n}_t] = \tilde{\mathbf{U}} + \tilde{\mathbf{F}}[\mathbf{n}_t]. \tag{10}$$

The matrices $\tilde{\mathbf{U}}$ and $\tilde{\mathbf{F}}$ can also be broken down into subprocesses (Figure 2), which represent different transition processes happening within each dimension:

$$\tilde{\mathbf{U}} = (\mathbf{K}_{b,p}\mathbf{K}_{s,b})^\top \mathbb{P}\mathbf{K}_{b,p}\mathbb{B}\mathbf{K}_{s,b}\mathbb{U}, \tag{11}$$

$$\tilde{\mathbf{F}}[\mathbf{n}_t] = (\mathbf{K}_{b,p}\mathbf{K}_{s,b})^\top \mathbb{M}\mathbf{K}_{b,p}\mathbb{H}[\mathbf{n}_t]\mathbf{K}_{s,b}\mathbb{R}. \tag{12}$$

The matrices $\mathbb{P}$, $\mathbb{B}$, $\mathbb{U}$, $\mathbb{M}$, $\mathbb{H}$ and $\mathbb{R}$ consist of block diagonal matrices with matrices $\mathbf{P}_{ij}$, $\mathbf{B}_{ik}$, $\mathbf{U}_{jk}$, $\mathbf{H}_{ij}$, $\mathbf{M}_{ik}$ and $\mathbf{R}_{jk}$ placed on the diagonal, respectively. The $\mathbf{K}$ matrices are vec-permutation matrices that

rearrange the structure of the **n** vector after each sub-process is applied, in order to align with the organization in the subsequent processes.

Equation (11) involves a series of operations on the population vector **n**. First, it is multiplied by the block matrix $\mathbb{U}$, which represents the stage within the breeding value within the phenotype. The resulting vector is then rearranged using the matrix $\mathbf{K}_{s,b}$. Next, it is multiplied by the matrix $\mathbb{B}$, which represents the breeding value within stage within the phenotype. Again, the resulting vector is rearranged, this time using the matrix $\mathbf{K}_{b,p}$. Finally, it is multiplied by the matrix $\mathbb{P}$, which represents the phenotype within the stage within the breeding value. The vector **n** is then rearranged back to its original structure, that is, stage within breeding value within phenotype, using the transpose of the product of matrices $\mathbf{K}_{b,p}$ and $\mathbf{K}_{s,b}$.

In Equation (12), the population vector **n** is subject to a comparable sequence of operations, although it involves distinct processes $\mathbb{R}$, $\mathbb{H}[\mathbf{n}_t]$ and $\mathbb{M}$ that serve, respectively, as substitutes for $\mathbb{U}$, $\mathbb{B}$ and $\mathbb{P}$. Each of these subprocesses is detailed in the following sections.

2.5.1 | Transition of living individuals

The transitions of living individuals from time t to time $t+1$ are captured by three sets of matrices, each of which represents a distinct process along a single dimension.

1. The stage transition matrices $\mathbf{U}_{jk}$ (dimension $s \times s$) capture the transition of individuals between juvenile and adult stages for each combination of breeding value j and phenotype k. Transitions between stages include survival S and maturation probabilities γ;

$$\mathbf{U}_{jk} = \begin{pmatrix} S_{J_{jk}}\left(1-\gamma_{jk}\right) & 0 \\ S_{J_{jk}}\gamma_{jk} & S_{A_{jk}} \end{pmatrix}, \tag{13}$$

where S_J and S_A are, respectively, the juvenile and adult survival rate corresponding to the breeding value j and phenotype class k.

2. The transition matrices for stage i and phenotypic class k, $\mathbf{B}_{i,k}$ (dimensions $b \times b$) contain transitions of the breeding value class for individuals in each stage i and phenotypic class k. Breeding values are assumed fixed from birth, hence $\mathbf{B}_{i,k}$ are identity matrices:

$$\mathbf{B}_{ik} = \begin{pmatrix} 1 & 0 & & 0 \\ 0 & \ddots & \ddots & \vdots \\ \vdots & \ddots & \ddots & 0 \\ 0 & & 0 & 1 \end{pmatrix}. \tag{14}$$

3. Transition matrices for stage i and breeding value class j, $\mathbf{P}_{i,j}$ (dimensions $p \times p$) contains transitions between phenotypic classes for individuals of stage i and in breeding value class j. Individuals are assumed to stay within their phenotypic class throughout their life, so that the matrices $\mathbf{P}_{i,j}$ are also identity matrices:

$$\mathbf{P}_{ij} = \begin{pmatrix} 1 & 0 & & 0 \\ 0 & \ddots & \ddots & \vdots \\ \vdots & \ddots & \ddots & 0 \\ 0 & & 0 & 1 \end{pmatrix}. \tag{15}$$

However, this assumption can be relaxed to account for phenotypic changes over an individual's lifetime, such as traits that improve with age.

2.5.2 | Production of new individuals

The production of new individuals with their own breeding values and phenotypes is represented by the following set of matrices:

1. Reproduction matrices ($\mathbf{R}_{jk}$) contain the state-specific fertilities of individuals within the breeding values and phenotypic classes j and k, respectively:

$$\mathbf{R}_{jk} = \begin{pmatrix} 0 & F_{jk} \\ 0 & 0 \end{pmatrix}, \tag{16}$$

where F is the fertility rate of adults carrying breeding value j and phenotype k.

2. The breeding values of newly produced offspring are determined by the matrices $\mathbf{H}_{i,k}[\mathbf{n}]$ (dimensions $b \times b$). Those matrices contain the probabilities that newly produced offspring receive a given breeding value depending on the breeding values of their parents and are assumed fixed across all i and k values.

   Individuals are assumed to reproduce sexually with random mating. The breeding values of the parents are denoted x_{j_f} and x_{j_m}. The breeding value of the offspring is sampled from a normal distribution with a mean equal to the average of the parental breeding values $\left(x_{j_f} + x_{j_m}\right)/2$ and a variance equal to half of $\mathbf{V}_A = h^2\mathbf{V}_P$. Here, h^2 represents the heritability of the phenotypic trait of interest in the population. This model is commonly referred to as the Fisher infinitesimal model (Bulmer, 1980; Fisher, 1918). We assumed that $\mathbf{V}_A$, $\mathbf{V}_P$ and h^2 at birth remain constant, even though the realized variance in breeding values and phenotypes among all living individuals may change over time. One could extend our model to incorporate variable $\mathbf{V}_A$, $\mathbf{V}_P$ and h^2 at birth. In particular, implementing a variable $\mathbf{V}_A$ would be straightforward and incur virtually no additional computational cost, as this parameter is not involved in computing the large matrices that dominate both computation time and memory usage. However, the dynamics of $\mathbf{V}_A$ depend on specific assumptions about genetic architecture (Walsh & Lynch, 2018), so we did not include this feature in our implementation.

   The probability that a mother with a breeding value in class j_f finds a male in class j_m and gives birth to an individual with a breeding value in class j is given by

$$G_{V_A}\left(x_j - \frac{x_{j_f} + x_{j_m}}{2}\right)\delta_{j_m}(\mathbb{R}\mathbf{n}), \tag{17}$$

where G_{V_A} represents the Gaussian distribution with a mean of 0 and a variance of $\frac{V_A}{2}$. The distribution is normalized so that its sum over breeding values j equals 1 for any parent's breeding values j_f and j_m. The function δ_{j_m} denotes the frequency of reproductive male individuals with a breeding value in class j_m within the population. We make the assumption that both males and females experience similar selective pressures and have an even sex ratio. Therefore, the frequency of alive reproductive males is equivalent to the frequency of alive reproductive females, which can be defined as follows:

$$\delta_{j_m}(\mathbb{R}\mathbf{n}) = \frac{\sum_{i,k=1}^{s,p} F_{j_m,k} n_{i,j_m,k}}{\sum_{i,j,k=1}^{s,b,p} F_{j,k} n_{i,j,k}}. \tag{18}$$

Then the transition matrices for a breeding value class j, $\mathbf{H}_{i,k}[\mathbf{n}]$ is defined for all breeding value classes j_f by

$$\left(\mathbf{H}_{i,k}[\mathbf{n}]\right)_{j,j_f} = \sum_{j_m=1}^{b} G_{V_A}\left(x_j - \frac{x_{j_f} + x_{j_m}}{2}\right)\delta_{j_m}(\mathbb{R}\mathbf{n}) \tag{19}$$

3. Matrices for stage i and breeding value class j, $\mathbf{M}_{i,j}$ (dimensions $p \times p$), assigns new offspring, with breeding value j, to their phenotypic class. The matrices $\mathbf{M}_{i,j}$ give the probability that a newborn with breeding value x_j will express the phenotype z_k at birth. Importantly, this probability is solely dependent on the breeding value of the newborn and is not influenced by the phenotype of the parent. For a newborn with breeding value class j, the probability to fall within the phenotypic class k is

$$G_{V_E}(z_k - x_j),$$

where G_{V_E} is the Gaussian distribution with mean 0 and variance $\mathbf{V}_E = \mathbf{V}_P - \mathbf{V}_A = (1 - h^2)\mathbf{V}_P$. The distribution is normalized so that its sum over phenotypes k equals 1 for any breeding values j. Thus the matrix $\mathbf{M}_{i,j}$, is defined by

$$\mathbf{M}_{ij} = \left(G_{V_E}(z_k - x_j)\right)_{k,l \in \{1,\ldots,p\}} \tag{20}$$

2.5.3 | Construction of block diagonal matrices

From the matrices $\mathbf{U}_{j,k}$, $\mathbf{R}_{j,k}$, $\mathbf{B}_{i,k}$, $\mathbf{H}_{i,k}$, $\mathbf{P}_{i,j}$ and $\mathbf{M}_{i,j}$, we construct block diagonal matrices; for example,

$$\mathbb{U} = \begin{pmatrix} \mathbf{U}_{11} & \mathbf{0} & \ldots & \mathbf{0} \\ \mathbf{0} & \mathbf{U}_{21} & \ldots & \mathbf{0} \\ \vdots & \vdots & \ddots & \vdots \\ \mathbf{0} & \mathbf{0} & \ldots & \mathbf{U}_{bp} \end{pmatrix}. \tag{21}$$

with similar block diagonal constructions for $\mathbb{R}$, $\mathbb{B}$, $\mathbb{H}$, $\mathbb{P}$ and $\mathbb{M}$.

3 | RESULTS

3.1 | Theoretical derivations of rates of adaptation

When selection acts through fertility F, that is, $F(z) = \exp(\log(F) + \beta z)$, the adaptation rates can be computed with respect to the parameters of our model. The selection gradient described by Equation (2) takes the form

$$\frac{\partial \ln(\bar{\lambda})}{\partial \bar{z}_t} = \frac{1}{\bar{\lambda}}\frac{\partial \bar{\lambda}}{\partial \bar{z}_t} = \frac{1}{\bar{\lambda}}\frac{\partial \bar{\lambda}}{\partial F}\frac{\partial F}{\partial \bar{z}_t}. \tag{22}$$

Using the sensitivity matrix $\mathbf{S}$ associated with the matrix $\left(\widetilde{\mathbf{U}} + \widetilde{\mathbf{F}}\right)$ and the generation time T, defined by Equation (4) then

$$\frac{\partial \bar{\lambda}}{\partial F} = \sum_{i_1,i_2=1}^{2} S_{i_1,i_2}\frac{\partial(\mathbf{R}+\mathbf{U})_{i_1,i_2}}{\partial F} = S_{1,2} = \frac{v_1 w_2}{v^T w}, \tag{23}$$

$$\frac{\partial F}{\partial \bar{z}_t}(0) = \beta F. \tag{24}$$

Equations (3) and (5) for the rate of adaptation become

$$\mathbf{RA_T} = h^2 \mathbf{V}_P \beta \frac{1}{T} \quad \text{and} \quad \mathbf{RA_G} = h^2 \mathbf{V}_P \beta. \tag{25}$$

Then, assuming similar selective pressure (β), heritability (h^2) and phenotypic variance ($\mathbf{V}_P$) among the five species, the adaptation rates per generation are also all equal. In contrast, the rate of adaptation per unit of time will decrease with the species' generation time.

When selection acts on fertility, the relative rate of change in fertility V_θ and the relative change in individual fitness V_{R_0} are equal

$$V_\theta = V_{R_0} = \beta.$$

The rates of adaptation measured in terms of unit of selection (6) and in terms of unit of individual selection (8) are equal

$$\mathbf{RA_{TS}}_\theta = \mathbf{RA_{TSR}}_0 = h^2 \mathbf{V}_P \frac{1}{T} \quad \text{and} \quad \mathbf{RA_{GS}}_\theta = \mathbf{RA_{GSR}}_0 = h^2 \mathbf{V}_P.$$

In addition, the rate of adaptation per generation and per unit of individual selection only depends on the heritability and the phenotypic variance, when selection acts on the fertility. The theoretical formulas for fertility, along with those for juvenile survival (S_J), maturation rate (γ) and adult survival (S_A) are provided in Table 2, and their derivations are detailed in Appendix S4.

3.2 | Method comparison

The adaptation rates per unit of time are almost identical in the three methods: theoretical derivations, IBM, or EvoDemo-Hyper MPM (Figure 3). Minor deviations between the theoretical derivations and MPM occur (e.g. species 1 in the juvenile survival selection scenario, Figure 3), validating our theoretical approximations. Although

TABLE 2 Rates of adaptation for different measures of time and different measures of selection when selection acts on different vital rate of the life cycle.

Rate	Fertility	Juvenile survival	Maturation	Adult survival
$\mathbf{RA_T}$	$h^2\mathbf{V}_P\beta\frac{1}{T}$	$h^2\mathbf{V}_P\beta\frac{1}{T}\frac{\lambda(1-S_J)}{\lambda-S_J(1-\gamma)}$	$h^2\mathbf{V}_P\beta\frac{1}{T}\frac{(\lambda-S_J)(1-\gamma)}{\lambda-S_J(1-\gamma)}$	$h^2\mathbf{V}_P\beta\frac{1}{T}\frac{S_A(1-S_A)}{\lambda-S_A}$
$\mathbf{RA_G}$	$h^2\mathbf{V}_P\beta$	$h^2\mathbf{V}_P\beta\frac{\lambda(1-S_J)}{\lambda-S_J(1-\gamma)}$	$h^2\mathbf{V}_P\beta\frac{(\lambda-S_J)(1-\gamma)}{\lambda-S_J(1-\gamma)}$	$h^2\mathbf{V}_P\beta\frac{S_A(1-S_A)}{\lambda-S_A}$
$\mathbf{RA_{TS\theta}}$	$h^2\mathbf{V}_P\frac{1}{T}$	$h^2\mathbf{V}_P\frac{1}{T}\frac{\lambda}{\lambda-S_J(1-\gamma)}$	$h^2\mathbf{V}_P\frac{1}{T}\frac{(\lambda-S_J)}{\lambda-S_J(1-\gamma)}$	$h^2\mathbf{V}_P\frac{1}{T}\frac{S_A}{\lambda-S_A}$
$\mathbf{RA_{GS\theta}}$	$h^2\mathbf{V}_P$	$h^2\mathbf{V}_P\frac{\lambda}{\lambda-S_J(1-\gamma)}$	$h^2\mathbf{V}_P\frac{(\lambda-S_J)}{\lambda-S_J(1-\gamma)}$	$h^2\mathbf{V}_P\frac{S_A}{\lambda-S_A}$
$\mathbf{RA_{TSR_0}}$	$h^2\mathbf{V}_P\frac{1}{T}$	$h^2\mathbf{V}_P\frac{1}{T}\frac{\lambda(1-S_J(1-\gamma))}{\lambda-S_J(1-\gamma)}$	$h^2\mathbf{V}_P\frac{1}{T}\frac{(\lambda-S_J)(1-S_J(1-\gamma))}{(1-S_J)(\lambda-S_J(1-\gamma))}$	$h^2\mathbf{V}_P\frac{1}{T}\frac{(1-S_A)}{\lambda-S_A}$
$\mathbf{RA_{GSR_0}}$	$h^2\mathbf{V}_P$	$h^2\mathbf{V}_P\frac{\lambda(1-S_J(1-\gamma))}{\lambda-S_J(1-\gamma)}$	$h^2\mathbf{V}_P\frac{(\lambda-S_J)(1-S_J(1-\gamma))}{(1-S_J)(\lambda-S_J(1-\gamma))}$	$h^2\mathbf{V}_P\frac{(1-S_A)}{\lambda-S_A}$

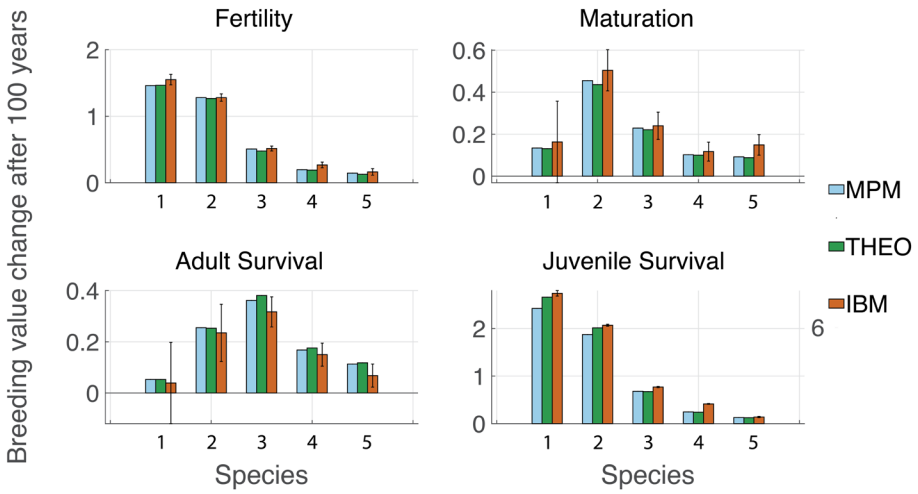

FIGURE 3 Comparison of the breeding value changes after 100 years for the three approaches: Theoretical derivations (THEO, green bars), Individual-Based Model (IBM, orange bars) and EvoDemo-Hyper Matrix Projection Model (MPM, blue bars). Theoretical derivations $\mathbf{RA_T}$ (THEO) are multiplied by 100 to match projection time of the IBM and MPM. Each panel corresponds to a particular vital rate under selection. Three bar sets illustrate the outcomes for each of the five species, arranged from the shortest to the longest generation time. Error bars for IBMs represent the 95% confidence interval for the mean of 100 simulation replicates. Note the difference in y-axis scales among panels. Table S1 details the values.

IBM results embody demographic stochasticity and genetic drift, they match the deterministic results on average. However, the confidence interval around the mean change in breeding value after 100 years tends to be larger for scenarios with lower rates of adaptation (Figure 3) because of lower population sizes and higher genetic drift occurring in those scenarios.

MPM results align with IBM as they cover the observed phenotypic and breeding value ranges over time. When observed values reach class boundaries, adaptation rates decrease (see the Appendix S3).

Computation times differ significantly between methods (see Appendix S5). Theoretical and MPM computations are fast (0.04 to 49 s), independent of species or vital rate. In contrast, IBM simulation times vary widely with scenarios and initial population size (1.45 to 18,500 s). Multiple IBM simulation runs (e.g. 100 replicates) are needed to estimate adaptation, affecting dynamics and extinction probability, amplifying differences from deterministic simulations.

3.3 | Definition comparison

Determining which species have the greatest adaptation capacity and identifying vital rates with the highest adaptation potential under similar selection pressures are essential questions. Our theoretical findings show that responses vary based on the adaptation rate definition. Adaptation rates differ among species and depend on the selected vital rate, all influenced by how the adaptation rate is defined.

The greatest differences in adaptation rate between species are found when adaptation is expressed per unit of time ($\mathbf{RA_T}$), compared to per unit of generation ($\mathbf{RA_G}$). The exception is when selection acts on adult survival (Figure 4). However, the pattern of variation in adaptation rates between species and vital rates remains consistent (top row on Figure 4), unless adaptation rates are calculated per selection units identified as the relative rate of change in an individual's fitness ($\mathbf{RA_{TS\theta}}$ and $\mathbf{RA_{TSR_0}}$, middle and bottom rows on Figure 4).

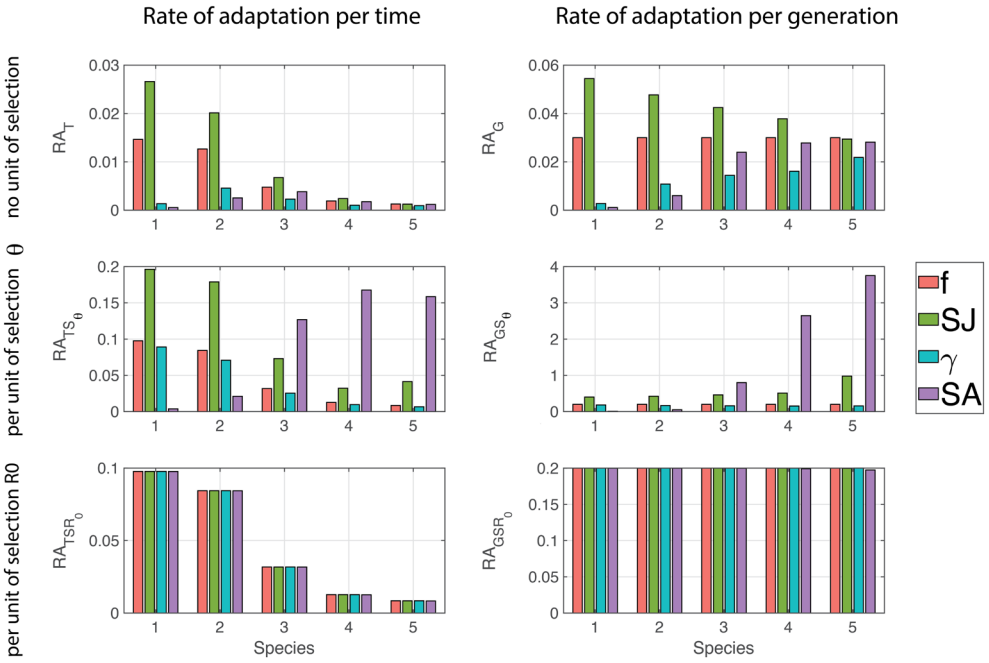

FIGURE 4 Comparison of adaptation rates based on the six definitions (Equations (3)–(5)–(6)–(8)). Each panel presents a different definition. The rate of adaptation can be indicated per unit of time $\mathbf{RA_T}$ (first column) or per unit of generation $\mathbf{RA_G}$ (second column). These rates can also be indicated per unit of selection (second and third row) or not (first row). The second row is represented by the unit of selection expressed by the relative rate of change in the vital rate θ: $\mathbf{RA_{TS\theta}}$ left column and $\mathbf{RA_{GS\theta}}$ right column. The third row corresponds to $\mathbf{RA_{TS_{R_0}}}$ (left column) and $\mathbf{RA_{GSR_0}}$ (right column), where the selection units are defined by the relative rate of change in an individual's fitness, quantified by the mean lifetime reproductive success R_0. The colour bar represents a specific vital rate that undergoes selection for the five species (x axis) arranged from the species with the shortest generation time to the species with the longest generation time.

For $\mathbf{RA_{TSR_0}}$ and $\mathbf{RA_{GSR_0}}$, there are no longer variations in the adaptation rates between the vital rates. Furthermore, when adjusted for generation time, adaptation rates are the same across all vital rates and species.

3.4 | Comparison of the rate at which organisms adapt across different life histories

The rate of adaptation per time $\mathbf{RA_T}$ is slower for species 5 than other species for all vital rates except adult survival. It decreases when the generation time increases if the pressure of selection acts on fecundity and juvenile survival. However, when the selection pressure acts on maturation rate and adult survival this monotonicity vanishes and intermediate species (2 and 3) have a more rapid rate of adaptation. Highest adaptation rates per time occur when selection acts on juvenile survival S_J, and remain high under fecundity selection. This pattern slightly differs for species 5, whose rate of adaptation is higher under fecundity selection (0.0013) than juvenile survival selection (0.0012). Furthermore, the main influence of juvenile survival is based on our assumption that the newborn survival rate S_0 equals the juvenile survival rate ($S_0 = S_J$). Under different assumptions and life cycle structures, adaptation rate per time may be greater when selection influences fecundity (Appendix S2).

The rate of adaptation per generation $\mathbf{RA_G}$ decreases along the slow-fast continuum if the pressure of selection acts on juvenile survival, but remains constant across species if it acts on fecundity. Furthermore, intermediate species (2 and 3) no longer have a faster rate of adaptation when selection pressure acts on the maturation rate or adult survival. Instead, the rate of adaptation per generation increases with the generation time when selection pressure acts on maturation and adult survival. Similarly to the adaptation rate per time, the adaptation rate per generation exhibits the highest values under juvenile survival selection and remains high when selection acts on fecundity, with a switch for species 5 (Figure 4).

The rates of adaptation per unit of vital rate over time $\mathbf{RA_{TS\theta}}$ exhibits a comparable trend to the rates of adaptation per time $\mathbf{RA_T}$ when selection influences fecundity and the survival of juveniles. However, it increases with the generation time when selection acts on adult survival and it decreases when selection pressure impacts the maturation rate. The highest $\mathbf{RA_{TS\theta}}$ values are still evident under juvenile survival selection in species 1 and 2. However, in species 3 to 5 the highest $\mathbf{RA_{TS\theta}}$ values occur under selection on adult survival. Differences in vital rates and species are comparable when the rates of adaptation per unit of vital rate are expressed in terms of generation time, $\mathbf{RA_{GS\theta}}$. However, adaptation rates exhibit significantly higher values when selection influences adult survival.

The rate of adaptation per unit of fitness over time $\mathbf{RA_{TSR_0}}$ shows no differences among the vital rates. Additionally, when the data is

normalized for generation time, the rate of adaptation $\mathbf{RA}_{\mathbf{GSR}_0}$ remains constant across both vital rates and species.

4 | DISCUSSION

Here, we present an EvoDemo-Hyper MPM that incorporates quantitative genetic processes to predict the evolution of breeding values and phenotypes within a population. We calculate theoretical adaptation rates using the Lande equation (Bulmer, 1980; Lande, 1976) and demonstrate that our theoretical predictions, along with simulation results from the MPM, align with those from a more conventional evolutionary IBM. This collaboration between evolutionary biologists and demographers highlighted different possible definitions of the rate of adaptation and their implications for comparing adaptation rates across life-history traits and species' generation times. We found no overarching prediction as to which species or life-history trait yields a higher rate of adaptation; this is contingent on the life cycle and the specific vital rates subject to selection pressure, as well as the choice of definition.

4.1 | Converging dynamics across diverse methodologies

The debates surrounding the use of evolutionary IPMs in the years 2010 (Chevin, 2015; Coulson et al., 2017; Hedrick et al., 2014; Janeiro et al., 2017; Pelletier, 2019; Traill et al., 2014; van Benthem et al., 2017) cast population matrix models against quantitative genetic models and may have suggested that one or the other approach was superior. Our work illustrates the rather self-evident fact that different approaches lead to similar results when they actually represent the same biological processes. In particular, population matrix models can incorporate quantitative trait inheritance correctly and thus provide consistent results with other methods.

While it is relatively trivial to create models of evolution and demography using IBMs or iterative equations, empirical applications remain relatively rare. Based on our own experience, we believe that it is in part because the range of possible models and assumptions is very large for any given system, requiring intense research to develop a useful empirical model. Furthermore, IBMs can be particularly long to develop, check and analyse (Grimm & Railsback, 2005; Grimm, 1999). Using a matrix projection model with a more constrained structure and ease of creation, for example, IPM, may be a good option to tackle evolution–demography questions.

Regrettably, the majority of IPMs that include evolutionary processes, subsequently referred to as EvoDemo-IPMs, have predominantly employed insufficient models for genetic transmission (Chevin, 2015; Janeiro et al., 2017). Most EvoDemo-IPMs incorrectly dampen evolutionary responses, or they introduce an unjustified environmental influence on inheritance (for instance see inheritance function in Clark-Wolf et al., 2024).

Integrating evolution in structured population models is not novel (Barfield et al., 2011; Childs et al., 2016; Coulson et al., 2017), but our EvoDemo-Hyper MPM is a rare option to include quantitative genetics accounting for two-sex inheritance while keeping a transparent and computationally efficient framework. Barfield et al. (2011) introduced a foundational model for evolution in stage-structured populations, extending Lande's theorem and Price's equation to this context. Their approach assumes that breeding values and phenotypes follow a joint normal distribution and primarily focuses on mean trait evolution using Lande's theorem. In contrast, our model relaxes the assumption of normality and explicitly tracks the full distribution of breeding values and phenotypes over time. This enables us to capture changes in both means and variances, which is particularly relevant when stabilizing selection under environmental change leads to non-Gaussian distributions (Garnier et al., 2023). Childs et al. (2016) and Coulson et al. (2017) later introduced a robust framework for EvoDemo-IPMs with quantitative genetic inheritance. Childs' approach explicitly tracks the full phenotype and breeding value separately, providing a direct representation of trait evolution. In contrast, Coulson's approach tracks the bivariate distribution of breeding values and environmental effects, offering greater flexibility for modelling plasticity and non-genetic inheritance. Additionally, Coulson's model inherently allows for two-sex inheritance, whereas Childs' does not include sex differences by default. While these previous models rely on integral-based formulations, our approach employs a matrix-based framework, which enhances computational efficiency and tractability. This allows for greater flexibility in model implementation and scalability, making our framework a practical alternative for integrating evolution into structured population models.

To our knowledge, Simmonds et al. (2020) is the only application of the proper EvoDemo-IPMs (Coulson et al., 2017), but it only incorporates the breeding values of the females within the inheritance function. Indeed, this model assumes that offspring breeding values are independent of paternal contributions, which, in the absence of stabilizing selection, may drive an increase in phenotypic variance over time. Furthermore, if environmental factors influence annual variations in the sex ratio of recruits by favouring males due to competitive advantages in resource-limited conditions, as suggested by Oddie (2000), excluding male contributions in the model may lead to biases in population estimates.

For simple applications, the analytical results we derived may prove particularly useful. The theoretical formulas allow us to compute adaptation rates for all species, vital rates and definitions within a short CPU time of 0.04 s. This paves the way for further theoretical exploration across a wider range of life histories, allowing for an examination of a more gradual spectrum of generation times.

4.2 | Which species adapt faster? And what is adaptation anyway?

Lots of research currently aims to assess the potential of species to adapt to rapid anthropogenic environmental change (Radchuk et al., 2019; Urban et al., 2023). More specifically, scientists and

wildlife managers would benefit from knowledge on the potential speed of adaptation of species to given selection pressure. Unfortunately, the present work shows that there cannot be a one-line answer to the question of which type of species will adapt slower or faster.

First, differences in the rates of adaptation among species do not always fall along a continuum. For instance, when using $\mathbf{RA_T}$, in the cases of maturation and adult survival, the highest rates are observed for species with intermediate generation times (Figure 4). The ordering of species from slowest to highest adaptation rate also varies depending on which vital rate is under selective pressure.

Furthermore, and perhaps more importantly, determining which species adapts faster depends on how we define the rate of adaptation. Throughout this work we highlighted two dimensions in the definition: the time unit and the measure of the strength of selection. Our six definitions provide dramatically different answers to which species, if any, adapts faster. Specifically, when defining adaptation using measures of selection on a linear scale ($\mathbf{RA_T}$ and $\mathbf{RA_G}$) or per unit of vital rate ($\mathbf{RA_{TS\theta}}$ and $\mathbf{RA_{GS\theta}}$), the variation in adaptation rates among species is contingent upon the particular vital rates targeted by selection. Thus determining which species adapt faster requires precise knowledge on selection pressure experienced by the species. The various perspectives on selection strengths and time units are not mutually exclusive; rather, they can be viewed as complementary strategies to take into account the effect of life history on adaptive dynamics. For example, an increase in mean survival rates will extend generation time, which consequently will slow down adaptation when measured per unit of vital rate and reduce selection pressure when measured per unit of fitness.

Our study does not explore another crucial aspect of variation in the definition of adaptation: whether it exclusively refers to genetic changes resulting from natural selection (as we assume in our work) or encompasses broader processes that enhance the expected population growth rate, such as adaptive phenotypic plasticity or some shifts in demographic structure. In evolutionary biology, adaptation (referring to adaptive evolution rather than the state of a trait being adaptive) is typically defined as an evolutionary response to natural selection. This distinction is important because alternative definitions can create apparent paradoxes in fundamental theorems of micro-evolution (Kokko, 2021). However, works on demography and wildlife management can adopt a broader definition of adaptation, encompassing any deterministic increase in population growth rate, including improvements in phenotypic plasticity and changes in stage structure (e.g. Clark-Wolf et al., 2024; Fox et al., 2019). Phenotypic plasticity, defined as the ability of a genotype to produce different phenotypes in response to environmental variation, can enable organisms to cope with environmental changes in the short term. For example, plasticity in the timing of breeding of great tits (*Parus major*) allows reducing mismatches between hatching and food availability under changing conditions (Simmonds et al., 2020). Our EvoDemo-Hyper model can easily be extended to incorporate phenotypic plasticity by defining non-trivial transition probabilities between phenotypic classes. This can be achieved through the transition matrices $\mathbf{P}_{i,j}$ (dimensions $p \times p$), which contain transitions between phenotypic classes for individuals of stage i with breeding value in class j.

The intricacy of defining adaptation is further complicated by sentences like 'adaptive change due to phenotypic plasticity', that raise ambiguity about whether phenotypic plasticity is a subset of adaptation or a distinct biological phenomenon. While we do not aim to prescribe one definition over another, we emphasize the importance of recognizing the diversity of definitions across disciplines and the potential for misunderstanding. Clarifying these distinctions is particularly relevant when designing studies or interpreting results across ecological and evolutionary research fields.

4.3 | Adapting to adaptation: How conservationists, demographers and geneticists define and measure change

Different definitions may be better suited depending on the scientific context. For instance, a conservation manager focused on implementing actions to aid species' adaptation over time might analyse adaptation rates per unit of time. They could observe that adaptation rates decline along the slow–fast continuum if selection pressure affects juvenile survival and fecundity. While the patterns become subtler when selection pressure impacts maturation and survival, there are no significant differences in adaptation rates overall. Consequently, conservation efforts might prioritize enhancing juvenile survival and fecundity in short-lived species and focus on any vital rates for longer-lived species to facilitate adaptation to global changes.

Demographers with an interest in life-history strategies might interpret the rate of adaptation per time per unit of selection in terms of its effect on the relative rate of change in an individual's vital rate. From this perspective, adaptation rates appear faster when selection impacts juvenile survival and fecundity, as well as maturation in short-lived species, whereas in long-lived species, adaptation is quicker when selection acts on adult survival.

Quantitative geneticists, on the other hand, prioritize the study of the causes and consequences of genetic change. They express adaptation rate per generation time and the response of selective pressure in standardized units of relative fitness or relative fitness components. Their approach is in line with the theoretical basis and conceptual focus on genetic change and is encapsulated by the breeder's equation. In one formulation, the breeder's equation expresses the per generation predicted change in the trait under selection as the product of additive genetic variance and a selection gradient (i.e. the average slope of relative fitness on the trait). When standardizing the response by the strength of selection, the predicted response depends only on additive genetic variance in the trait, which explains why the rate of adaptation $\mathbf{RA_{GSR_0}}$ is equal for all species and all vital rates on Figure 4. The actual standardized strength of selection does depend on the details of the life-history

and which fitness component selection acts on, but by measuring selection in a standardized way, quantitative genetics can take those details out of the equation. Instead of the details of life-history and on which fitness component selection acts, quantitative geneticists therefore stress the importance of differences in generation time, strength of selection and additive genetic variance (or, equivalently, heritabilities) across species (e.g. Carlson et al., 2014; Kingsolver et al., 2012; Postma, 2014).

5 | CONCLUSIONS

Our results validate the EvoDemo-Hyper MPM as a robust framework for modelling evolutionary and demographic dynamics. Compared to Individual-Based Models, it offers greater tractability and computational efficiency while capturing the full distribution of breeding values and phenotypes over time. Ultimately, the choice of method may depend on factors such as computational efficiency, the researcher's background in evolution or demography and the level of detail required to represent the life cycle. We also highlight that patterns observed among species and vital rates are influenced by definitions, underscoring the importance of maintaining awareness of this context when drawing broad conclusions about species adaptation, particularly in response to global changes. Overall, we recommend researchers interested in which species adapt faster in a given scenario not to assume an answer based on some verbal expectation, but instead to model the rate of adaptation with the definition that matters to them and find out a quantitative answer.

AUTHOR CONTRIBUTIONS

Timothée Bonnet, Jimmy Garnier, Stephanie Jenouvrier and Joanie Van de Walle contributed equally to all aspects of this research. This work reflects a collaborative and interdisciplinary effort, in which all authors were involved in: *Conceptualization*: Timothée Bonnet, Jimmy Garnier, Stephanie Jenouvrier and Joanie Van de Walle. *Formal analysis*: Timothée Bonnet, Jimmy Garnier, Stephanie Jenouvrier and Joanie Van de Walle. *Investigation*: Timothée Bonnet, Jimmy Garnier, Stephanie Jenouvrier and Joanie Van de Walle. *Methodology*: Timothée Bonnet, Jimmy Garnier, Stephanie Jenouvrier and Joanie Van de Walle. *Visualization*: Timothée Bonnet, Jimmy Garnier, Stephanie Jenouvrier and Joanie Van de Walle. *Writing*: Timothée Bonnet, Jimmy Garnier, Stephanie Jenouvrier and Joanie Van de Walle. *Project administration*, *supervision and submission*: Stephanie Jenouvrier.

ACKNOWLEDGEMENTS

This work was supported by the National Science Foundation under Grant No. ORCC NSF 2222057 No NSFGEO-NERC 1951500.

CONFLICT OF INTEREST STATEMENT

The authors declare that there are no conflicts of interest regarding the publication of this paper.

PEER REVIEW

The peer review history for this article is available at https://www.webofscience.com/api/gateway/wos/peer-review/10.1111/2041-210X.70075.

DATA AVAILABILITY STATEMENT

All of the MATLAB and R code for building the EvoDemo-Hyper MPM and the Individual-Based Model are provided on https://github.com/fledge-whoi/Eco-EvoHyperstateModel (fixed version). The R code for the EvoDemo-Hyper MPM is also provided as an R package at https://src.koda.cnrs.fr/timotheebonnet/evodemohypermpm.git (version meant to be developed further). The codes to reproduce the results and figures of our study can be found at https://doi.org/10.5281/zenodo.15236774 (Bonnet et al., 2025).

ORCID

Joanie Van de Walle https://orcid.org/0000-0002-5137-1851
Jimmy Garnier https://orcid.org/0000-0002-0145-1028
Timothée Bonnet https://orcid.org/0000-0001-7186-5288
Stephanie Jenouvrier https://orcid.org/0000-0003-3324-2383

REFERENCES

Barfield, M., Holt, R. D., & Gomulkiewicz, R. (2011). Evolution in stage-structured populations. *The American Naturalist*, *177*, 397–409.

Bellard, C., Bertelsmeier, C., Leadley, P., Thuiller, W., & Courchamp, F. (2012). Impacts of climate change on the future of biodiversity. *Ecology Letters*, *15*, 365–377.

Berteaux, D., Réale, D., McAdam, A. G., & Boutin, S. (2004). Keeping pace with fast climate change: Can Arctic life count on evolution? 1. *Integrative and Comparative Biology*, *44*, 140–151.

Bienvenu, F., & Legendre, S. (2015). A new approach to the generation time in matrix population models. *The American Naturalist*, *185*, 834–843.

Bonnet, T., Garnier, J., & Jenouvrier, S. (2025). Toward a unified approach to modeling adaptation among demographers and evolutionary ecologists. *Zenodo*, https://doi.org/10.5281/zenodo.15236774

Bulmer, M. G. (1980). *The mathematical theory of quantitative genetics*. Clarendon Press.

Carlson, S. M., Cunningham, C. J., & Westley, P. A. H. (2014). Evolutionary rescue in a changing world. *Trends in Ecology & Evolution*, *29*, 521–530.

Caswell, H. (2000). *Matrix population models* (Vol. *1*). Sinauer.

Chevin, L. M. (2015). Evolution of adult size depends on genetic variance in growth trajectories: A comment on analyses of evolutionary dynamics using integral projection models. *Methods in Ecology and Evolution*, *6*, 981–986.

Chevin, L. M., Collins, S., & Lefèvre, F. (2012). Phenotypic plasticity and evolutionary demographic responses to climate change: Taking theory out to the field. *Functional Ecology*, *27*, 967–979.

Childs, D. Z., Sheldon, B. C., & Rees, M. (2016). The evolution of labile traits in sex- and age-structured populations. *Journal of Animal Ecology*, *85*, 329–342.

Clark-Wolf, T. J., Boersma, P. D., Plard, F., Rebstock, G. A., & Abrahms, B. (2024). Increasing environmental variability inhibits evolutionary rescue in a long-lived vertebrate. *Proceedings of the National Academy of Sciences of the United States of America*, *121*, e2406314121.

Compagnoni, A., Levin, S., Childs, D. Z., Harpole, S., Paniw, M., Römer, G., Burns, J. H., Che-Castaldo, J., Rüger, N., Kunstler, G., Bennett, J. M., Archer, C. R., Jones, O. R., Salguero-Gómez, R., & Knight, T. M. (2021). Herbaceous perennial plants with short generation time

have stronger responses to climate anomalies than those with longer generation time. *Nature Communications*, *12*, 1824.

Coste, C. F., & Pavard, S. (2020). Analysis of a multitrait population projection matrix reveals the evolutionary and demographic effects of a life history trade-off. *Ecological Modelling*, *418*, 108–915.

Coulson, T., Kendall, B. E., Barthold, J., Plard, F., Schindler, S., Ozgul, A., & Gaillard, J.m. (2017). Modeling adaptive and nonadaptive responses of populations to environmental change. *The American Naturalist*, *190*, 313–336.

de Villemereuil, P., Schielzeth, H., Nakagawa, S., & Morrissey, M. (2016). General methods for evolutionary quantitative genetic inference from generalized mixed models. *Genetics*, *204*, 1281–1294.

Doak, D. F., & Morris, W. F. (2010). Demographic compensation and tipping points in climate-induced range shifts. *Nature*, *467*, 959–962.

Easterling, M. R., Ellner, S. P., & Dixon, P. M. (2000). Size-specific sensitivity: Applying a new structured population model. *Ecology*, *81*, 694–708.

Falconner, D. S., & Mackay, T. F. C. (1996). *Introduction to quantitative genetics* (4th ed.). Pearson.

Fisher, R. A. (1918). The correlation between relatives on the supposition of Mendelian inheritance. *Transactions of the Royal Society of Edinburgh*, *52*, 399–433.

Fisher, R. A. (1930). *The genetical theory of natural selection*. Oxford University Press.

Fox, R. J., Donelson, J. M., Schunter, C., Ravasi, T., & Gaitán-Espitia, J. D. (2019). Beyond buying time: The role of plasticity in phenotypic adaptation to rapid environmental change. *Philosophical Transactions of the Royal Society, B: Biological Sciences*, *374*, 20180174.

Garnier, J., Cotto, O., Bouin, E., Bourgeron, T., Lepoutre, T., Ronce, O., & Calvez, V. (2023). Adaptation of a quantitative trait to a changing environment: New analytical insights on the asexual and infinitesimal sexual models. *Theoretical Population Biology*, *152*, 1–22.

Gonzalez, A., Ronce, O., Ferrière, R., & Hochberg, M. (2013). Evolutionary rescue: An emerging focus at the intersection between ecology and evolution. *Philosophical Transactions of the Royal Society of London. Series B, Biological Sciences*, *368*, 20120404.

Grimm, V. (1999). Ten years of individual-based modelling in ecology: What have we learned and what could we learn in the future? *Ecological Modelling*, *115*, 129–148.

Grimm, V., & Railsback, S. F. (2005). Introduction. In *Individual-based modeling and ecology* (pp. 15–21). Princeton University Press.

Haaland, T. R., Payo-Payo, A., Acker, P., Fortuna, R., Burthe, S. J., Ratikainen, I. I., Daunt, F., & Reid, J. M. (2023). Eco-evolutionary dynamics of partially migratory metapopulations in spatially and seasonally varying environments. *bioRxiv*, https://doi.org/10.1101/2023.11.28.568986

Hedrick, P. W., Coltman, D. W., Festa-Bianchet, M., & Pelletier, F. (2014). Not surprisingly, no inheritance of a trait results in no evolution. *Proceedings of the National Academy of Sciences of the United States of America*, *111*, 4810.

Hunter, C. M., & Caswell, H. (2005). The use of the vec-permutation matrix in spatial matrix population models. *Ecological Modelling*, *188*, 15–21.

Janeiro, M. J., Coltman, D. W., Festa-Bianchet, M., Pelletier, F., & Morrissey, M. B. (2017). Towards robust evolutionary inference with integral projection models. *Journal of Evolutionary Biology*, *30*, 270–288.

Jenouvrier, S., Long, M. C., Coste, C. F. D., Holland, M., Gamelon, M., Yoccoz, N. G., & Sæther, B. E. (2022). Detecting climate signals in populations across life histories. *Global Change Biology*, *28*, 2236–2258.

Jenouvrier, S., & Visser, M. E. (2011). Climate change, phenological shifts, eco-evolutionary responses and population viability: Toward a unifying predictive approach. *International Journal of Biometeorology*, *55*, 905–919.

Kendall, B. E., Fujiwara, M., Diaz-Lopez, J., Schneider, S., Voigt, J., & Wiesner, S. (2019). Persistent problems in the construction of matrix population models. *Ecological Modelling*, *406*, 33–43.

Kingsolver, J. G., Diamond, S. E., Siepielski, A. M., & Carlson, S. M. (2012). Synthetic analyses of phenotypic selection in natural populations: Lessons, limitations and future directions. *Evolutionary Ecology*, *26*, 1101–1118.

Kokko, H. (2021). The stagnation paradox: The ever-improving but (more or less) stationary population fitness. *Proceedings of the Royal Society B: Biological Sciences*, *288*, 20212145.

Lachs, L., Bozec, Y. M., Bythell, J. C., Donner, S. D., East, H. K., Edwards, A. J., Golbuu, Y., Gouezo, M., Guest, J. R., Humanes, A., Riginos, C., & Mumby, P. J. (2024). Natural selection could determine whether Acropora corals persist under expected climate change. *Science*, *386*, 1289–1294.

Lamarins, A., Fririon, V., Folio, D., Vernier, C., Daupagne, L., Labonne, J., Buoro, M., Lefèvre, F., Piou, C., & Oddou-Muratorio, S. (2022). Importance of interindividual interactions in eco-evolutionary population dynamics: The rise of demo-genetic agent-based models. *Evolutionary Applications*, *15*, 1988–2001.

Lande, R. (1976). Natural selection and random genetic drift in phenotypic evolution. *Evolution*, *30*, 314–334.

Lande, R. (1979). Quantitative genetic analysis of multivariate evolution, applied to brain: Body size allometry. *Evolution*, *33*, 402–416.

Lynch, M., & Walsh, B. (1998). *Genetics and analysis of quantitative traits*. Sinauer Associates.

Neubert, M. G., & Caswell, H. (2000). Density-dependent vital rates and their population dynamic consequences. *Journal of Mathematical Biology*, *41*, 103–121.

Oddie, K. R. (2000). Size matters: Competition between male and female great tit offspring. *Journal of Animal Ecology*, *69*, 903–912.

Paniw, M., Ozgul, A., & Salguero-Gómez, R. (2018). Interactive life-history traits predict sensitivity of plants and animals to temporal autocorrelation. *Ecology Letters*, *21*, 275–286.

Parmesan, C., & Yohe, G. (2003). A globally coherent fingerprint of climate change impacts across natural systems. *Nature*, *421*, 37–42.

Pelletier, F. (2019). Testing evolutionary predictions in wild mice. *Science*, *363*, 452–453.

Postma, E. (2014). Four decades of estimating heritabilities in wild vertebrate populations: Improved methods, more data, better estimates? In A. Charmentier, D. Garant, & L. E. B. Kruuk (Eds.), *Quantitative genetics in the wild* (1st ed., pp. 16–33). Oxford University Press.

Postuma, M., Schmid, M., Guillaume, F., Ozgul, A., & Paniw, M. (2020). The effect of temporal environmental autocorrelation on eco-evolutionary dynamics across life histories. *Ecosphere*, *11*, e03029.

Queller, D. C. (2017). Fundamental theorems of evolution. *The American Naturalist*, *189*, 345–353.

Radchuk, V., Reed, T., Teplitsky, C., Pol, M.v.d., Charmantier, A., Hassall, C., Adamík, P., Adriaensen, F., Ahola, M. P., Arcese, P., Avilés, J. M., Balbontin, J., Berg, K. S., Borras, A., Burthe, S., Clobert, J., Dehnhard, N., Lope, F.d., Dhondt, A. A., … Kramer-Schadt, S. (2019). Adaptive responses of animals to climate change are most likely insufficient. *Nature Communications*, *10*, 1–14.

Rees, M., & Ellner, S. P. (2019). Why so variable: Can genetic variance in flowering thresholds be maintained by fluctuating selection? *The American Naturalist*, *194*, E13–E29.

Roth, G., & Caswell, H. (2016). Hyperstate matrix models: Extending demographic state spaces to higher dimensions. *Methods in Ecology and Evolution*, *7*, 1438–1450.

Salguero-Gómez, R. (2017). Applications of the fast–slow continuum and reproductive strategy framework of plant life histories. *New Phytologist*, *213*, 1618–1624.

Salguero-Gómez, R., Jones, O. R., Jongejans, E., Blomberg, S. P., Hodgson, D. J., Mbeau-Ache, C., Zuidema, P. A., de Kroon, H., & Buckley, Y. M. (2016). Fast–slow continuum and reproductive strategies structure

plant life-history variation worldwide. *Proceedings of the National Academy of Sciences of the United States of America*, *113*, 230–235.

Simmonds, E. G., Cole, E. F., Sheldon, B. C., & Coulson, T. (2020). Testing the effect of quantitative genetic inheritance in structured models on projections of population dynamics. *Oikos*, *129*, 559–571.

Traill, L. W., Schindler, S., & Coulson, T. (2014). Demography, not inheritance, drives phenotypic change in hunted bighorn sheep. *Proceedings of the National Academy of Sciences of the United States of America*, *111*(13), 13,223–13,228.

Urban, M. C., Swaegers, J., Stoks, R., Snook, R. R., Otto, S. P., Noble, D. W. A., Moiron, M., Hällfors, M. H., Gómez-Llano, M., Fior, S., Cote, J., Charmantier, A., Bestion, E., Berger, D., Baur, J., Alexander, J. M., Saastamoinen, M., Edelsparre, A. H., & Teplitsky, C. (2023). When and how can we predict adaptive responses to climate change? *Evolution Letters*, *8*, 172–187.

van Benthem, K. J. V., Bruijning, M., Bonnet, T., Jongejans, E., Postma, E., & Ozgul, A. (2017). Disentangling evolutionary, plastic and demographic processes underlying trait dynamics: A review of four frameworks. *Methods in Ecology and Evolution*, *8*, 75–85.

Vedder, O., Bouwhuis, S., & Sheldon, B. C. (2013). Quantitative assessment of the importance of phenotypic plasticity in adaptation to climate change in wild bird populations. *PLoS Biology*, *11*, e1001605.

Walsh, B., & Lynch, M. (2018). Short-term changes in the variance: 1. Changes in the additive variance. In *Evolution and selection of quantitative traits* (pp. 549–572). Oxford University Press.

Xuereb, A., Rougemont, Q., Tiffin, P., Xue, H., & Phifer-Rixey, M. (2021). Individual-based eco-evolutionary models for understanding adaptation in changing seas. *Proceedings of the Royal Society B: Biological Sciences*, *288*, 20212006.

SUPPORTING INFORMATION

Additional supporting information can be found online in the Supporting Information section at the end of this article.

Appendix S1: Individual-based model.

Appendix S2: Comparison of life cycle.

Appendix S3: Comparison of additive variance and functional relationships of the phenotypes.

Appendix S4: Theoretical adaptation rates of the different vital rates.

Appendix S5: Computation time.

How to cite this article: Van de Walle, J., Garnier, J., Bonnet, T., & Jenouvrier, S. (2025). Toward a unified approach to modelling adaptation among demographers and evolutionary ecologists. *Methods in Ecology and Evolution*, *00*, 1–14. https://doi.org/10.1111/2041-210X.70075